Heat transfer coefficients under dry- and wet-surface conditions for a spirally coiled finned tube heat exchanger☆

Paisarn Naphon, Somchai Wongwises*

Fluid Mechanics, Thermal Engineering and Multiphase Flow Research Laboratory (FUTURE), Department of Mechanical Engineering, King Mongkut's University of Technology Thonburi, 91 Suksawas Road, Bangmod, Bangkok 10140, Thailand

Abstract

In the present study, the average tube-side and air-side heat transfer coefficients in a spirally coiled finned tube heat exchanger under dry- and wet-surface conditions are experimentally investigated. The test section is a spiral-coil heat exchanger, which consists of six layers of concentric spirally coiled tube. Each tube is fabricated by bending a 9.6-mm outside diameter straight copper tube into a spiral coil of four turns. Aluminium fins with thickness 0.6 mm and outside diameter 28.4 mm are placed helically around the tube. The chilled water and the hot air are used as working fluids. The test runs are done at the air and water mass flow rates ranging between 0.02 and 0.2 kg/s and between 0.04 and 0.25 kg/s, respectively. The inlet-air and -water temperatures are between 35 and 60 °C and between 10 and 35 °C, respectively. The effects of the inlet conditions of both working fluids flowing through the heat exchanger on the heat transfer coefficients are discussed. New correlations based on the data gathered during this work for predicting the tube-side and air-side heat transfer coefficients for the spirally coiled finned tube heat exchanger are proposed.

Keywords: Heat transfer; Spirally coiled finned tube heat exchanger; Aluminium fins

1. Introduction

As fluid flows through curved tubes, due to the curvature of the tubes, a secondary flow induced by the generated centrifugal force has significant ability to enhance the heat transfer rate. Heat transfer and flow characteristics in the curved tubes have been studied by a number of researchers. Goering and Humphrey [1] solved the fully elliptic Navier–Stokes and energy equations to analyze the effects of buoyancy and curvature on the fully developed laminar flow through a heated horizontal curved. Yang et al. [2] studied the effects of the flow rate, the Prandtl number, the pipe-period and the pipe-amplitude on the heat transfer for a laminar flow in a pipe with periodically varying finite curvature. Nigam et al. [3] solved the governing equations of fully developed laminar flow and heat transfer of Newtonian and power law fluids in the thermal entrance region of curved tubes for analyzing the secondary velocity profile, temperature profile and Prandtl number. The mathematical model for turbulent flow based on the equations of conservation of mass, momentum and energy was solved by Targett et al. [4]. They studied the fully developed angular flow and fully developed convection in the annulus between two concentric cylinders. Li et al. [5] applied the renormalization group (RNG) k–ϵ model for considering the three-dimensional turbulent mixed convective heat transfer. Yang and Chiang [6] studied the effects of the Dean number, Prandtl number, Reynolds number and the curvature ratio on the heat transfer for periodically varying-curvature curved-pipe inside a larger diameter straight pipe to form a double-pipe heat exchanger. Suga [7] presented a two-component limit turbulence model and the wall reflection free model. The results showed that the two-component limit turbulence model was reliable in the case of strong curvature. Wang and Cheng [8] numerically studied the combined free and forced convective heat transfer in a rotating curved circular tube with uniform wall heat flux and peripherally uniform wall temperature.

Investigation on the heat transfer characteristics of spiral-coil heat exchangers has received comparatively little attention in literature. The most productive studies were continuously carried out by Ho et al. [9] and Ho and Wijeysundera [10,11]. They applied the correlations of the tube-side and air-side heat transfer coefficients reported in literature to determine the thermal performance of the spiral coil heat exchanger under cooling and dehumidifying conditions. Experiments were performed to verify the simulation results. Later, Naphon and Wongwises [12] modified the mathematical model of Ho and Wijeysundera [11] by including the fin efficiency and using the other existing heat transfer coefficient correlations. The results were compared with Ho et al.'s measured data. Recently, in order to solve the lack of the appropriate heat transfer coefficient correlations for the spirally coiled configuration, Naphon and Wongwises [13] proposed a correlation for the average in-tube heat transfer coefficient for a spiral-coil heat exchanger under wet-surface conditions. The experiments with the same experimental apparatus were also conducted under dry-surface conditions and the average inside and outside heat transfer coefficients were proposed (Naphon and Wongwises [14]).

To the best of authors' knowledge, none of these papers presents the heat transfer coefficients associated with the sides in the spirally coiled finned tube heat exchanger under dry- and wet-surface conditions. In the present study, the main concern is to propose the inside and outside heat transfer coefficients for the tube of the spirally coiled finned tube heat exchanger under dry- and wet-surface conditions. Correlations in the practical form are developed from all experimental data for predicting the heat transfer coefficients.

2. Experimental apparatus and method

A schematic diagram of the experimental apparatus is shown in Fig. 1. The test loop consists of a test section, refrigerant loop, chilled water loop, hot air loop and data acquisition system. The water and air are used as working fluids. The test section is a spirally coiled finned tube heat exchanger, which consists of a shell and spiral coil unit. The test section and the connections of the piping system are designed such that parts can be changed or repaired easily. In addition to the loop components, a full set of instruments for measuring and control of temperature and flow rate of all fluids is installed at all important points in the circuit.

Air is discharged by a centrifugal blower into the channel and is passed through a straightener, heater, guide vane, test section and then discharged to the atmosphere. The speed of the centrifugal blower is controlled by the inverter. Air velocity is measured by a hot wire anemometer. The test channel is fabricated from zinc, with an inner diameter of 300 mm and a length of 12 m. It is well-insulated by an insulator with a thickness of 6.4 mm. The hot air flows into the center core and then flows across the spiral coils, radially outwards to the inner wall of the shell before leaving the heat exchanger at the air outlet section. The inlet temperature of the air is raised to the desired level by using electric heaters controlled by a temperature controller. The inlet- and outlet-air temperatures are measured by eight type-T copper-constantan thermocouples. The inlet and outlet relative humidities of air are detected by humidity transmitters.

The chilled water loop consists of a 0.3-m^3 storage tank, an electric heater controlled by adjusting the voltage, a stirrer and a cooling coil immerged inside a storage tank. R22 is used as the refrigerant for chilling the water. After the temperature of the water is adjusted to the desired level, the chilled water is pumped out of the storage tank, and is passed through a filter, flow meter, test section and returned to the storage tank. The flow rate of the water is measured by a flow meter with a range of 0–10 GPM.

The spirally coiled finned tube heat exchanger consists of a steel shell and a spirally coiled finned tube unit. The spiral-coil unit consists of six layers of the spirally coiled finned tube. Each tube is

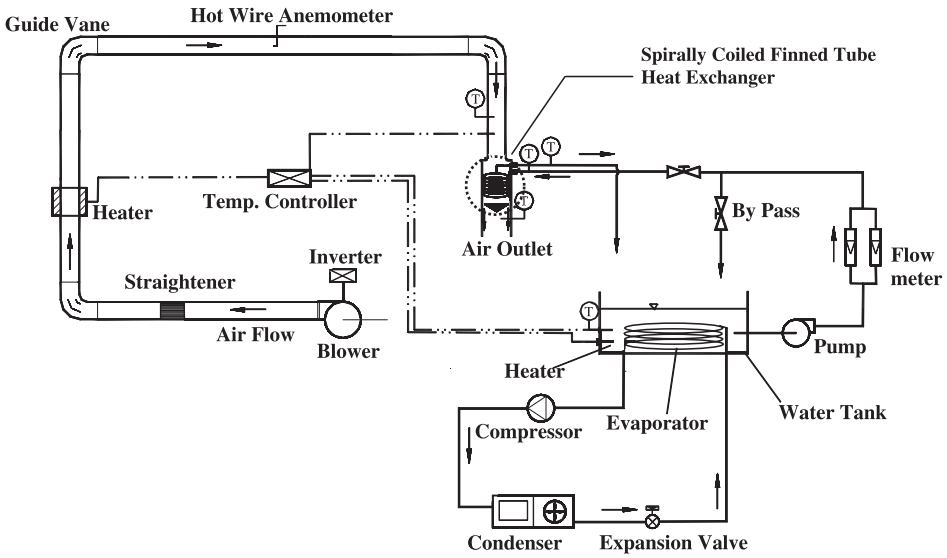

Fig. 1. Schematic diagram of experimental apparatus.

Table 1
Dimensions of the spirally coiled finned tube heat exchanger

Parameters	Dimensions
Outer diameter of tube, mm	9.6
Inner diameter of tube, mm	8.7
Innermost diameter of spiral coil, mm	145.0
Outermost diameter of spiral coil, mm	350.4
Number of coil turns	4
Number of spiral coils	6
Diameter of shell, mm	430
Distance between layer, mm	31.7
Length of shell, mm	350
Diameter of hole at air inlet, mm	125
Diameter of closed plate at air outlet, mm	360
Fin pitch, mm	3.1
Fin height, mm	9.4
Fin thickness, mm	0.6
Number of fins per metre	310

fabricated by bending a 9.6-mm outside diameter straight copper tube into a spiral coil of four turns with the innermost and outermost diameters of 145.0 and 350.4 mm, respectively. Aluminium fins with thickness 0.6 mm and outside diameter 28.4 mm are placed helically around the copper tube. Two vertical manifold tubes with outer diameters of 28.5 mm are used to connect each end of the spirally coiled finned tube. The measuring positions are concentrated at the third layer of the spirally coiled finned tube unit from the uppermost layer. The distribution temperatures of the water and tube surface are measured in five positions along the spiral coil with 1-mm diameter probes extending inside the tube and mounted on the tube wall surface in which the water flows. The dimensions of the spirally coiled finned tube heat exchanger are listed in Table 1.

Experiments were conducted with various temperatures and flow rates of hot air and chilled water entering the test section. In the experiments, the chilled water flow rate was increased in small increments while the hot air flow rate, inlet chilled water and hot air temperatures were kept constant. The flow rate of hot air was controlled by adjusting the speed of the centrifugal blower. An inverter was used to control the speed of the motor for driving the blower. The inlet hot air and chilled water temperatures were adjusted to the desired level by using electric heaters controlled by temperature controllers. The system was allowed to approach the steady state before any data were recorded. The steady state condition was reached when the temperature and flow rates at all measuring points were no longer fluctuating. After stabilization, the variables at the locations mentioned above were recorded.

3. Data reduction

The data reduction of the measured results is summarized in the following procedures.
Heat transferred to the chilled water in the test section, Q_w, can be calculated from

$$Q_w = m_w C_{p,w}\left(T_{w,out} - T_{w,in}\right) \quad (1)$$

where m_w is the total mass flow rate of water, $C_{p,w}$ is the specific heat of water, $T_{w,in}$ and $T_{w,out}$ are the inlet- and outlet-water temperatures, respectively.

For dry-surface conditions, heat transferred from the hot air, Q_a, can be calculated from

$$Q_a = m_a C_{p,a}\left(T_{a,in} - T_{a,out}\right) \tag{2}$$

where m_a is the total air mass flow rate, $C_{p,a}$ is the specific heat of air, $T_{a,in}$ and $T_{a,out}$ are the inlet- and outlet-air temperatures, respectively.

However, when moist air passes over a cooling coil having a surface temperature below its dew-point, the air is chilled and condensed. In this case, the heat transferred from the hot air can be calculated from:

$$Q_a = m_a\left(i_{a,in} - i_{a,out}\right) \tag{3}$$

where $i_{a,in}$ and $i_{a,out}$ are the inlet enthalpy and outlet enthalpy of moist air and are defined by:

$$i_a = C_{p,a}T_a + \omega_a i_g. \tag{4}$$

The total heat transfer rate, Q_{total}, used in the calculation is determined from the air-side and water-side as follows:

$$Q_{total} = \frac{Q_a + Q_w}{2}. \tag{5}$$

The tube-side heat transfer coefficient for the spirally coiled finned tube, h_i, can be calculated from the average heat transfer rate obtained from

$$Q_{ave} = \frac{Q_{total}}{6} = h_i A_i\left(T_{s,ave} - T_{w,ave}\right) \tag{6}$$

where $T_{s,ave}$ is the average wall temperature and $T_{w,ave}$ is the average water temperature. The inside surface area, A_i, is of one spirally coiled finned tube, which can be obtained from

$$A_i = (2\pi r_i)\sum_{n=1}^{4}(2\pi R_n) \tag{7}$$

where

$$R_n = [R_{min} + (2n-1)\alpha\pi] \tag{8}$$

where R_{min} is the minimum spiral-coil radius, r_i is the inner radius of the tube, n is the coil turn number and α is the rate of change of radius.

The overall heat transfer coefficient can be determined from

$$Q_{\text{ave}} = U_{\text{i}} A_{\text{i}} (F) \Delta T_{\text{LMTD}} \tag{9}$$

where ΔT_{LMTD} is the logarithmic-mean temperature difference, F is the correction factor, which is equal to 1 for this case.

An air-side heat transfer coefficient, h_{o}, is usually obtained from the overall thermal resistance consisting of three resistances in series: the convective resistance on the inner surface of the curved pipe, conductance resistance of the pipe wall and the convective resistance on the outer surface of the curved pipe:

$$\frac{1}{U_{\text{i}} A_{\text{i}}} = \frac{1}{\eta_{\text{o}} h_{\text{o}} A_{\text{o}}} + \frac{\delta_{\text{t}}}{k_{\text{t}} A_{\text{ave}}} + \frac{1}{h_{\text{i}} A_{\text{i}}}. \tag{10}$$

The overall surface efficiency, η_{o}, defined as the ratio of the effective heat transfer area to the total heat transfer area can be expressed in term of fin efficiency, η, fin surface area, A_{f}, and total outside surface area, A_{o}, as follows:

$$\eta_{\text{o}} = 1 - \frac{A_{\text{f}}}{A_{\text{o}}} (1 - \eta). \tag{11}$$

The fin efficiency, η, is determined by the method proposed by Schmidt [15] as follows:

$$\eta = \frac{\tanh(M r_{\text{o}} \phi)}{M r_{\text{o}} \phi} \tag{12}$$

where

$$\phi = \left(\frac{R_{\text{f}}}{r_{\text{o}}} - 1 \right) \left[1 + 0.35 \ln \left(\frac{R_{\text{f}}}{r_{\text{o}}} \right) \right] \tag{13}$$

$$M^2 = \frac{2 h_{\text{o}}}{k_{\text{f}} \delta_{\text{f}}}. \tag{14}$$

For wet-surface conditions, M^2 is determined by the method developed by McQuiston and Parker [16] as follows:

$$M^2 = \frac{2 h_{\text{o}}}{k_{\text{f}} \delta_{\text{f}}} \left(1 + \frac{B_{\text{sa}} i_{\text{fg}}}{C_{\text{p,a}}} \right) \tag{15}$$

$$B_{\text{sa}} = \frac{\omega_{\text{sat,ave}} - \omega_{\text{a,ave}}}{T_{\text{sat,ave}} - T_{\text{a,ave}}} \tag{16}$$

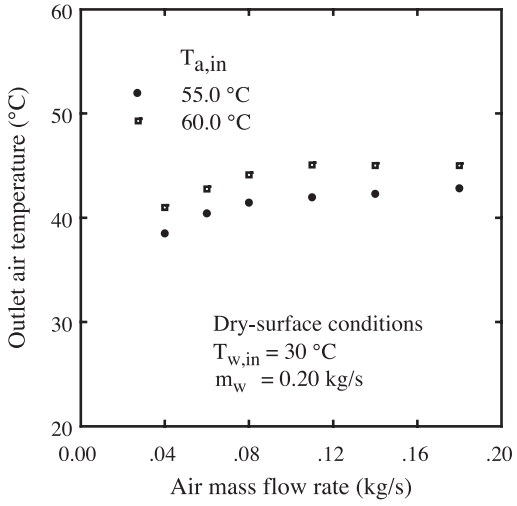

Fig. 2. Variation of $T_{a,out}$ with m_a.

where R_f is the fin radius, r_o is the outer tube radius, k_f is the thermal conductivity of the fin, δ_f is the fin thickness, $T_{a,ave}$ is the average temperature of air, $\omega_{a,ave}$ is the average specific humidity of air and $T_{sat,ave}$ is the saturated temperature of the water film which is equal to the average wall temperature, $T_{s,ave}$.

The specific humidity of air at saturated conditions, $\omega_{sat,s}$, is a function of the tube wall temperature and can be obtained from the correlation given by Liang et al. [17].

$$\omega_{sat,ave} = \left(3.7444 + 0.3078T_{s,ave} + 0.0046T_{s,ave}^2 + 0.0004T_{s,ave}^3\right)10^{-3}. \quad (17)$$

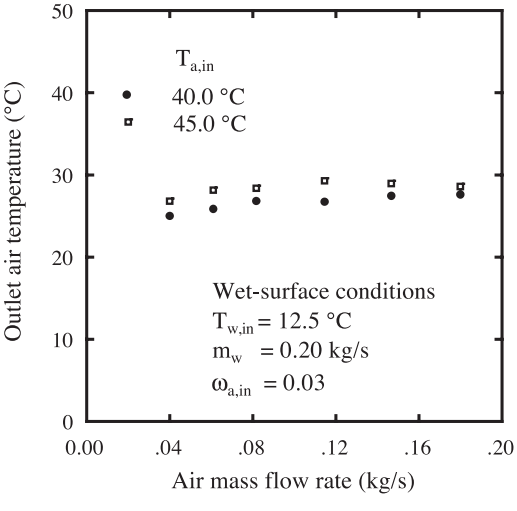

Fig. 3. Variation of $T_{a,out}$ with m_a.

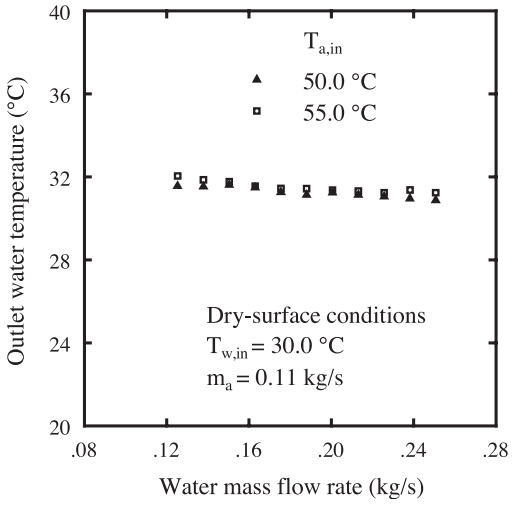

Fig. 4. Variation of $T_{w,out}$ with m_w.

To obtain the air-side heat transfer coefficient and the overall surface efficiency, an iterative procedure is employed to solve Eqs. (10)–(17). The air-side heat transfer characteristics of the heat exchanger are presented in the following form

$$j = \left(\frac{h_o}{G_{max} C_{p,a}}\right) Pr^{2/3}. \tag{18}$$

4. Results and discussion

Figs. 2 and 3 show the variation of the outlet-air temperature with air mass flow rate for different inlet-air temperatures under dry- and wet-surface conditions, respectively. The outlet-air temperature

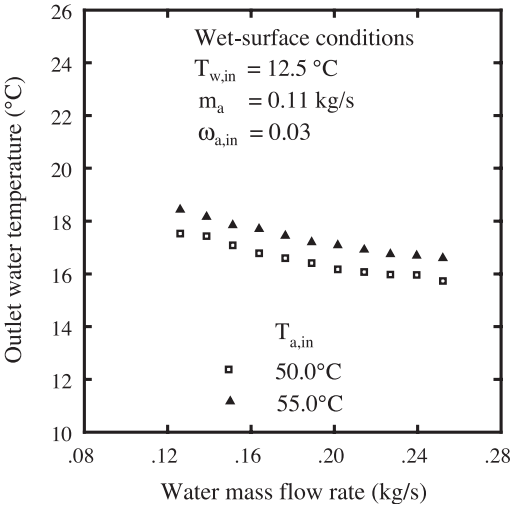

Fig. 5. Variation of $T_{w,out}$ with m_w.

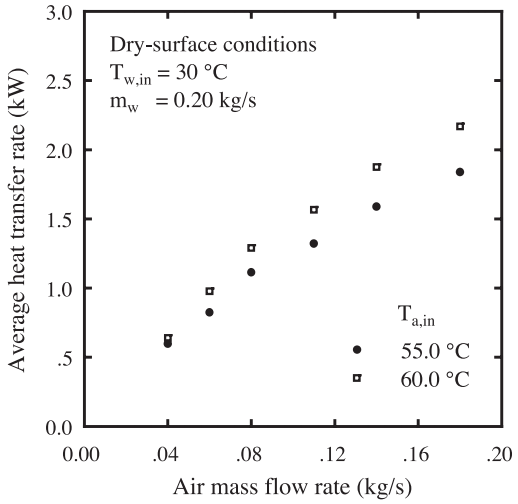

Fig. 6. Variation of Q with m_a.

tends to increase while the air mass flow rate increases. However, when the air mass flow rate is over 0.1 kg/s, a further increase of the air mass flow rate does not seem to increase the outlet-air temperature.

Figs. 4 and 5 illustrate the variation of the outlet-water temperatures with water mass flow rate for different inlet-air temperatures under dry- and wet-surface conditions, respectively. It is found that, when the inlet-air and -water temperatures, and air mass flow rate are kept constant, the outlet-water temperature decreases with increasing water mass flow rate. However, for dry-surface conditions, increase of water mass flow rate gives a slightly lower outlet-water temperature across the range of water

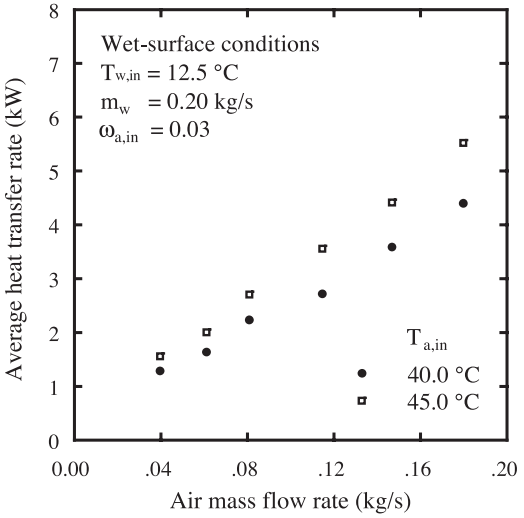

Fig. 7. Variation of Q with m_a.

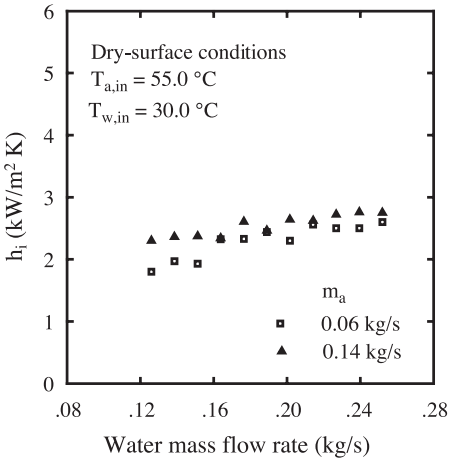

Fig. 8. Variation of h_i with m_w.

mass flow rate. Moreover, it seems that for dry-surface conditions, the inlet-air temperature has less significant effect on the outlet-water temperature.

Figs. 6 and 7 show the variation of the average heat transfer rate with air mass flow rate for the different inlet-air temperatures under dry- and wet-surface conditions, respectively. As shown, at a specific temperature of air entering the heat exchanger, the heat transfer rate increases with increasing air mass flow rate. Also, at the same air mass flow rate, the heat transfer rates at higher inlet-air temperatures are higher than those at lower ones across the range of air mass flow rate. The effect of the inlet-air temperature on the average heat transfer rate can be clearly seen at higher air mass flow rate.

Figs. 8 and 9 show the variation of the average tube-side heat transfer coefficients calculated from the data obtained from the present experiment with water mass flow rate at various air mass flow rates. As

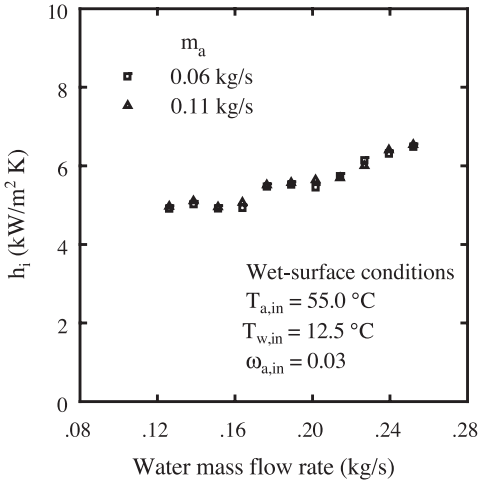

Fig. 9. Variation of h_i with m_w.

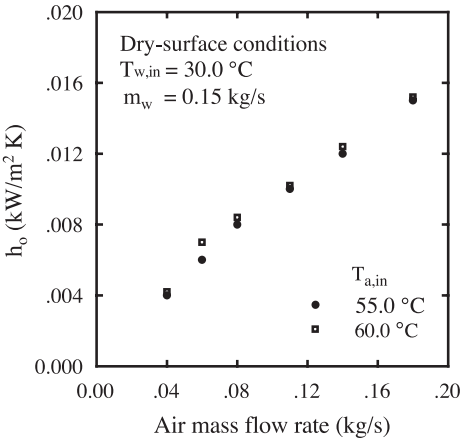

Fig. 10. Variation of h_o with m_a.

expected, the average tube-side heat transfer coefficient increases with increasing water mass flow rate. This is because the heat transfer coefficient depends directly on the heat removal capacity of the chilled water. In addition, at a given water mass flow rate, the average tube-side heat transfer coefficients for higher air mass flow rate are higher than those for lower ones.

Figs. 10 and 11 show the variation of the out-side heat transfer coefficient with air mass flow rate for different inlet-air temperatures. The out-side heat transfer coefficient increases rapidly with air mass flow rate. It can be noted that the inlet-air temperature has an insignificant effect on the out-side heat transfer coefficient.

Based on the present data, the tube-side heat transfer coefficient and out-side heat transfer coefficient are proposed in term of the Nusselt number and the Colburn j factor. The correlations are of the form:

For dry-surface conditions:

$$Nu = \frac{h_i d_i}{k} = 4.0 De^{0.464} Pr^{-0.755} \tag{19}$$

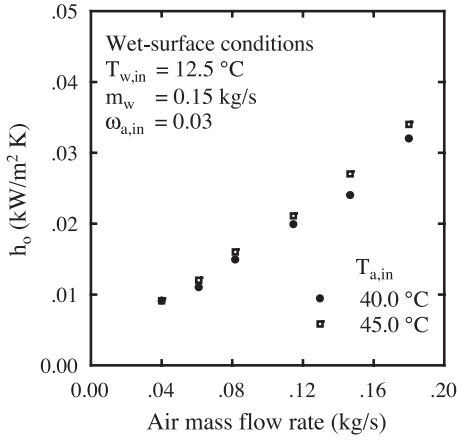

Fig. 11. Variation of h_o with m_a.

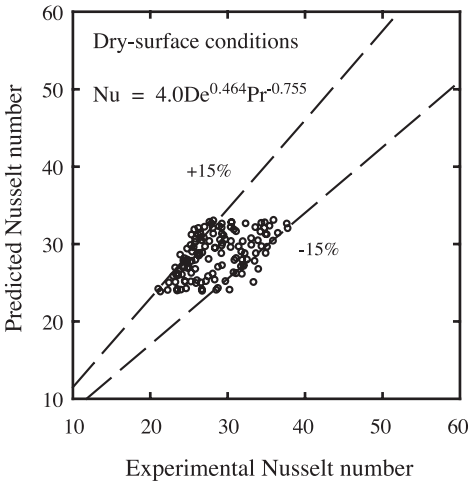

Fig. 12. Comparison of Nu.

where $200 \leq De \geq 3000$, $Pr > 5$

$$j = \frac{h_o}{G_{max} C_{p,a}} Pr^{2/3} = 0.0178 Re_o^{-0.239} \tag{20}$$

where $Re_o < 4000$.

For wet-surface conditions:

$$Nu = \frac{h_i d_i}{k} = 19.0 De^{0.464} Pr^{-0.755} \tag{21}$$

where $200 \leq De \geq 3000$, $Pr > 7$.

$$j = \frac{h_o}{G_{max} C_{p,a}} Pr^{2/3} = 0.029 Re_o^{-0202} \tag{22}$$

where $Re_o < 4000$.

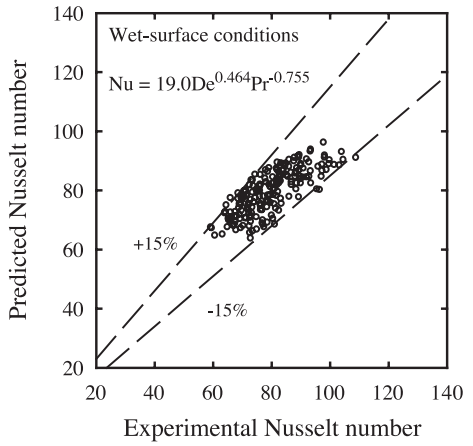

Fig. 13. Comparison of Nu.

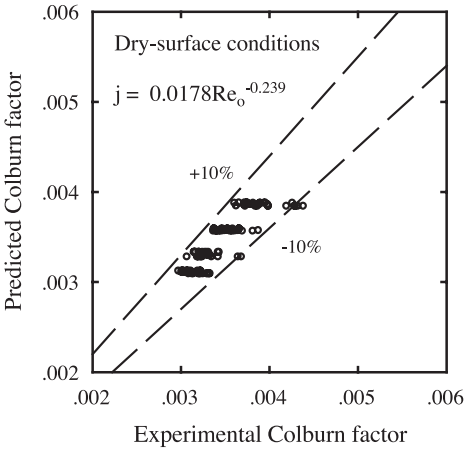

Fig. 14. Comparison of j factor.

Comparisons between the Nusselt numbers obtained from the present experiments with those calculated from the proposed correlations are shown in Figs. 12 and 13, for dry- and wet-surface conditions, respectively. It can be clearly seen from these figures that the majority of the data falls within $\pm 15\%$ of the proposed correlations. Comparisons of the Colburn j factor obtained from the experiment with those calculated by the proposed correlations are shown in Figs. 14 and 15. It can be noted that the values obtained from the correlations are consistent with the experimental data and lie within $\pm 10\%$ for the dry-surface conditions and $\pm 15\%$ for the wet-surface conditions. It is quite difficult to compare the results between dry- and wet-surface conditions because the experimental conditions are different. However, it can be clearly seen from the correlations obtained that both tube-side heat transfer coefficient and out-side heat transfer coefficient under wet-surface conditions are higher than those under dry-surface conditions.

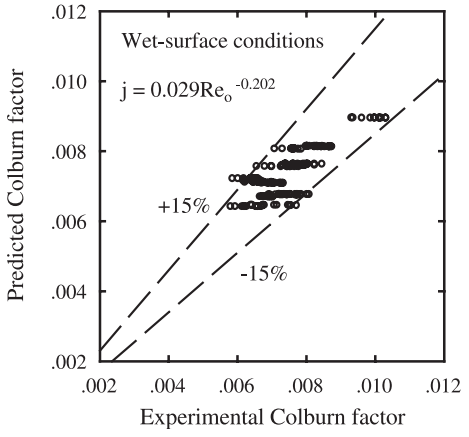

Fig. 15. Comparison of j factor.

5. Conclusions

This paper presents new heat transfer data of a spirally coiled finned tube heat exchanger under dry- and wet-surface conditions. The heat exchanger consists of six layers of concentric spirally coiled finned copper tube, each with four turns. Aluminium fins are placed helically around the tube. The effects of relevant parameters are investigated. New proposed correlations based on the present experimental data are given for practical uses.

Nomenclature

A	area, m^2
d	tube diameter, m
i	enthalpy, kJ/kg
Nu	Nussult number
R	spiral-coil radius, m
r	tube radius, m
η	fin efficiency
α	radius change per radian, m/radian
C_p	specific heat, kJ/(kg K)
F	correction factor
j	Colburn j factor
Pr	Prandtl number
Re	Reynolds number
T	temperature, °C
η_o	overall surface efficiency
De	Dean number
G	mass flux, kg/m^2 s
m	mass flow rate, kg/s
Q	heat transfer rate, W
R_f	fin radius, m
ω	specific humidity
δ	thickness, m

Subscripts

a	air
g	gas
max	maximum
o	outside
sat	saturated
ave	average
i	inside
min	minimum
out	outlet
t	tube

f fin
in inlet
n number of coil turn
s wall, surface
w water

Acknowledgments

The authors would like to express their appreciation to the Thailand Research Fund (TRF) for providing financial support for this study.

References

[1] D. Goering, J.A.C. Humphrey, Int. J. Heat Mass Transfer 40 (1997) 2187.
[2] R. Yang, S.F. Chang, W. Wu, Int. Commun. Heat Mass Transf. 27 (2000) 133.
[3] K.D.P. Nigam, S. Agawal, V.K. Srivastava, Chem. Eng. J. 84 (2001) 223.
[4] M.J. Targett, W.B. Retallick, S.W. Churchill, Int. J. Heat Mass Transf. 38 (1995) 1989.
[5] L.J. Li, C.X. Lin, M.A. Ebadian, Int. J. Heat Mass Transfer 41 (1998) 3793.
[6] R. Yang, F.P. Chaing, Int. J. Heat Mass Transfer 45 (2002) 3199.
[7] K. Suga, Int. J. Heat Mass Transfer 46 (2003) 161.
[8] L. Wang, K.C. Cheng, Int. J. Heat Mass Transfer 39 (1996) 3381.
[9] J.C. Ho, N.E. Wijeysundera, S. Rajasekar, T.T. Chandratilleke, Heat Recovery Syst. CHP 15 (1995) 457.
[10] J.C. Ho, N.E. Wijeysundera, Appl. Therm. Eng. 16 (1996) 777.
[11] J.C. Ho, N.E. Wijeysundera, Appl. Therm. Eng. 19 (1999) 865.
[12] P. Naphon, S. Wongwises, J. Eng. Phys. Thermophys. 76 (2003) 71.
[13] P. Naphon, S. Wongwises, Int. Commun. Heat Mass Transf. 29 (2002) 797.
[14] P. Naphon, S. Wongwises, Experimental and theoretical investigation of the heat transfer characteristics and performance of a spiral-coil heat exchanger under dry-surface conditions, 2nd International Conference on Heat Transfer, Fluid Mechanics, and Thermodynamics, 24–26 June, Victoria Falls, Zambia, 2003.
[15] T.E. Schmidt, Refrig. Eng. 49 (1949) 351.
[16] F.C. McQuiston, J.D. Parker, Heating, Ventilating and Air-Conditioning, 4th edition, Wiley, New York, 1994.
[17] S.Y. Liang, M. Liu, T.N. Wong, G.K. Nathan, Appl. Therm. Eng. 19 (1999) 1129.